

# NEXT LEVEL: PURSUING SUSTAINABILITY UNDER ENERGY EARTHSHOTS — PERSPECTIVE



## Multiscale approaches for optimizing the impact of strain on Na-ion battery cycle life

**Michael J. Brady**, and **Jessica L. Andrews**, Department of Chemistry, University of Southern California, Los Angeles, CA 90089, USA

**Andrea Zambotti**, Department of Materials Science and Engineering, University of California, Los Angeles, Los Angeles, CA 90095, USA

**Delin Zhang**, Department of Aerospace and Mechanical Engineering, University of Southern California, Los Angeles, CA 90089, USA

**Xintong Yuan** Department of Chemical and Biomolecular Engineering, University of California, Los Angeles, Los Angeles, CA 90095, USA

**Kodi Thurber**, Department of Chemistry and Biochemistry, University of California, Los Angeles, Los Angeles, CA 90095, USA

**Xiangfeng Duan**, Department of Chemistry and Biochemistry, University of California, Los Angeles, Los Angeles, CA 90095, USA; The California NanoSystems Institute, University of California, Los Angeles, Los Angeles, CA 90095, USA

**Yuzhang Li**, Department of Chemical and Biomolecular Engineering, University of California, Los Angeles, Los Angeles, CA 90095, USA

**Johanna Nelson Weker**, Stanford Synchrotron Radiation Lightsource, SLAC National Accelerator Laboratory, Menlo Park, CA 94025, USA

**Ananya Renuka Balakrishna**, Materials Department and Materials Research Laboratory, University of California, Santa Barbara, Santa Barbara, CA 93106, USA

**Kimberly A. See**, Division of Chemistry and Chemical Engineering, California Institute of Technology, Pasadena, CA 91125, USA

**Ram Seshadri** and **Anton Van der Ven**, Materials Department and Materials Research Laboratory, University of California, Santa Barbara, Santa Barbara, CA 93106, USA

**Bruce S. Dunn**, Department of Materials Science and Engineering, University of California, Los Angeles, Los Angeles, CA 90095, USA; The California NanoSystems Institute, University of California, Los Angeles, Los Angeles, CA 90095, USA

**Sarah H. Tolbert** , Department of Materials Science and Engineering, University of California, Los Angeles, Los Angeles, CA 90095, USA; Department of Chemistry and Biochemistry, University of California, Los Angeles, Los Angeles, CA 90095, USA; The California NanoSystems Institute, University of California, Los Angeles, Los Angeles, CA 90095, USA

**Brent C. Melot**, Department of Chemistry, University of Southern California, Los Angeles, CA 90089, USA; Department of Chemical Engineering and Materials Science, University of Southern California, Los Angeles, CA 90089, USA

Address all correspondence to Sarah H. Tolbert at [tolbert@chem.ucla.edu](mailto:tolbert@chem.ucla.edu); Brent C. Melot at [melot@usc.edu](mailto:melot@usc.edu)

(Received: 20 June 2024; accepted: 24 October 2024; published online: 26 November 2024)

## ABSTRACT

*Understanding the fundamental way materials respond to localized strains at the atomic length-scale is a critical first step in the development of highly reversible, long cycle life, Na-ion insertion hosts. This perspective explores a variety of methods that can be employed to mitigate the detrimental effects of large strain. The insights gained from these investigations should help lay the foundation for the creation of more economical and sustainable batteries that could have immediate impact on global energy infrastructure.*

The high costs and geopolitical challenges inherent to the lithium-ion (Li-ion) battery supply chain have driven a rising interest in the development of sodium-ion (Na-ion) batteries as a potential alternative. Unfortunately, the larger ionic radius of Na limits the reversibility of cycling because of the extensive atomic rearrangements that accompany Na-ion insertion, which in turn limit diffusion and charging speed, and lead to rapid degradation of the electrodes. The Center for Strain Optimization for Renewable Energy (STORE) was established to address these challenges and develop new electrode materials for Na-ion cells. This article discusses the current state-of-the-art materials used in Na-ion cells and several directions that STORE believes are critical to understand and control the structural and volumetric changes during the reversible (de)insertion of large cations.

**Keywords** Energy storage · Na · Stress/strain relationship · Intercalation · Layered · Amorphous

## Introduction

As society races to establish a net zero-emission economy by 2050, the need to accelerate the introduction of renewable power sources into the grid is becoming more urgent. A critical part of this effort will require the deployment of robust, affordable, and sustainable energy storage solutions. In recognition of these challenges, the Department of Energy recently set a target of \$0.05/kWh for long-duration energy storage (LDES), which will require diverse collections of technologies. Within this portfolio, secondary batteries based on the reversible (de)insertion of ions are poised to play an important role in grid leveling by providing a rapid response to supply disruptions.

However, the high costs and geopolitical challenges associated with the Li-ion battery supply chain pose severe challenges for large-scale incorporation into the grid. One proposed solution is to simply replace Li with more naturally abundant Na. Unfortunately, the larger ionic radius of Na ions (see Fig. 1) offsets this benefit because the extensive atomic rearrangements that currently accompany Na-ion diffusion cause rapid electrode degradation, thereby limiting the cycling lifetime. Thus, while Na-ion cells should, in principle, be cheaper to produce, they

remain significantly more expensive than Li-ion systems when amortized over the lifetime of the battery. To mitigate this issue, a fundamental understanding of how materials respond to the strain generated during Na-ion (de)insertion is critical for their continued development and deployment.

With this in mind, a team of faculty members from across southern California came together to establish the Center for Strain Optimization for Renewable Energy (STORE), which was recently funded by the Science Foundations for Energy Earthshots (SFEE) program of the US Department of Energy. The team consists of an interdisciplinary group of scientists and engineers with proficiency in both computation and experiments, and broad expertise in electrochemical energy storage. The complementary nature of the team includes research experience in solid-state chemistry, nanomaterials, electrochemical methods, ex situ and operando structural characterization, and atomistic and multiscale modeling. The goal of this perspective is to discuss the current state-of-the-art materials used in Na-ion cells and present several directions that the STORE center will pursue to manipulate and control structural and volumetric changes in electrode materials during the reversible (de)insertion of large cations.

## Discussion

Although there is near universal agreement that electrochemical energy storage must be an integral part of a green-energy future, there is less agreement about how to reduce the cost of energy storage. Replacing high-cost lithium-ion cells with lower-cost sodium-ion batteries is one option frequently considered in future energy models, but the details of what can be achieved with optimized sodium cell performance remains unclear. Here we posit that developing methods to mitigating strain on the electrode particle length scale is a key factor for achieving long-cycle-life sodium-ion batteries. Mitigating strain on the atomic scale suppress electrode-level volume change. Allowing for fast cycling in materials without the problems of electrode cracking or delamination. We further posit that understanding volume change in sodium-ion electrodes at a fundamental level will lead to the designing new sodium-ion electrode materials that will allow for efficient, stable, lower-cost energy storage.

Michael J. Brady and Jessica L. Andrews have contributed to this work equally and are sharing the first author position.

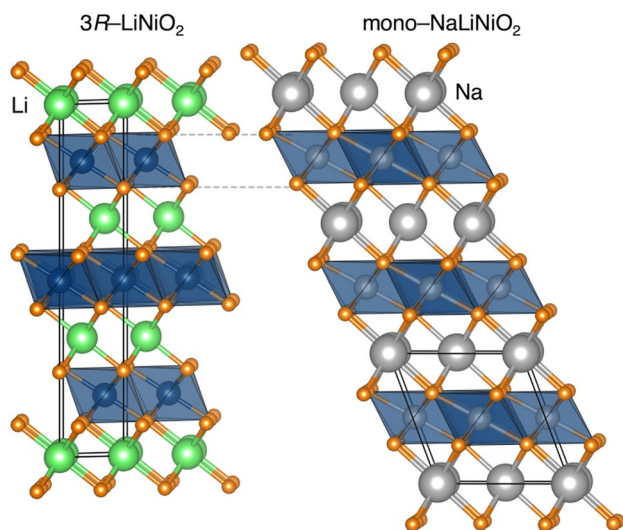


**Figure 1.** Illustration of  $\text{LiNiO}_2$  and  $\text{NaNiO}_2$ , drawn to scale, to highlight the difference in size of the transition-metal layer spacing resulting from the larger Na ionic radius.

### State-of-the-art

In research that parallels the extensive work on cathodes for Li-ion cells, layered transition metal oxides, such as  $\text{Na}_x\text{CoO}_2$ , have been thoroughly explored as candidate Na-ion cathode materials. Practical capacities between 70 and 100 mAh/g have been reported, but they fall short of the theoretical maximum of 213 mAh/g.<sup>1</sup> These phases are known to exhibit poor stability over extended cycling, particularly at reasonable rates, with only 68% capacity retention after 40 cycles at 2C. This is generally attributed to the poor reversibility of the glide transformations that occur during (de)sodiation, driven by the large ionic radius of Na (see Fig. 1).<sup>2</sup> Other layered oxides, such as  $\text{Na}_x\text{MnO}_2$ , exhibit a practical capacity of 163 mAh/g, which is much closer to the theoretical capacity of 170 mAh/g. However, the long-term cycling performance remains poor, with only 77% capacity retention after 50 cycles.<sup>3</sup> Alleviating the strain introduced by these structural transformations is critical to expanding the capacity and extending the lifetime of Na-ion cathodes. For example, recent studies have focused on suppressing these transitions in the layered oxides through methods such as the introduction of ‘locking layers’<sup>4</sup> or chemical doping to create rigid pillars to anchor the layers together.<sup>5</sup> Transition metal sulfides are also interesting sodium layered insertion hosts. A recent study suggests that introducing a small amount of tensile strain into these 2D-layered transition metal sulfides can greatly increase the amount of sodium inserted.<sup>6</sup> However, these materials typically generate tiny cracks or defects to reduce the strain produced by sodium intercalation.<sup>7</sup> Therefore, heterostructuring transition metal sulfides to have larger interlayer spacings than the bare materials is one proposed strategy to mitigate these detrimental effects.<sup>8–13</sup>

In recent years, several polyanionic compounds have been explored. NASICON-structured  $\text{Na}_3\text{V}_2(\text{PO}_4)_3$  has a practical capacity of 85 mAh/g, which is short of the already low theoretical

capacity of 118 mAh/g, although its stability during cycling is somewhat better.<sup>14</sup>  $\text{NaVPO}_4\text{F}$  is also of interest, however, it suffers from low electronic conductivity like many other polyanionic compounds. While the addition of graphene has been shown to enhance its performance, with the composite exhibiting 121 mAh/g with good retention over 50 cycles at C/20, its capacity decreases significantly at C/2.<sup>15</sup> Despite the lower capacity exhibited by these polyanion compounds, they remain an area of active research in part due to their high operating potentials as a result of inductive effects. Current work shows that vanadium is critical for controlling strain in polyanionic compounds due to its ability to adopt several oxidation states and to use local strain to satisfy its valence, rather than long-range structural distortions or large volume expansions.<sup>16</sup> Interestingly, the  $\text{Na}^+$  migration barriers of some olivine-based compounds, like  $\text{NaFePO}_4$ , are significantly reduced when tensile strain is applied in the *ac*-plane.<sup>17</sup> Balancing the mitigation of large-scale strain, while taking advantage of local strain-enhanced conductivity is an exciting area for advancing polyanion cathodes for Na-ion batteries.

Transition metal hexacyanometalates frameworks derived from  $\text{Fe}_4[\text{Fe}(\text{CN})_6]_3$ , commonly known as Prussian Blue or Prussian Blue Analogs (PBAs), have also been utilized and appear more promising. For example, the Fe-based PBA  $\text{KFe}_2(\text{CN})_6$  exhibits a practical reversible capacity of approximately 100 mAh/g (compared to a theoretical capacity of  $\sim 175$  mAh/g), but only when cycled at a relatively slow rate of C/20.<sup>18</sup> Despite this rate limitation,  $\text{KFe}_2(\text{CN})_6$  showed 99% capacity retention after 30 cycles, a promising capability ascribed to the material’s open framework with large tunnels for easier ion transport.<sup>18</sup> This suggests that the most promising candidates for Na-ion cathodes will require structural motifs containing large channels capable of accommodating Na (de)intercalation without generating a large amount of strain in the crystal structure. However, the identities of the transition metals within the PBA structure also plays a critical role in the amount of strain produced during electrochemical cycling. For example, while Mn-based PBAs are promising due to their higher operating potentials, the Jahn-Teller distortion upon oxidation to  $\text{Mn}^{3+}$  results in significantly increased lattice strain.<sup>19</sup> Recent studies have shown that reducing structural defects, such as  $[\text{Fe}(\text{CN})_6]^{4-}$  vacancies and coordinated water,<sup>20</sup> as well as  $\text{Ni}^{2+}$  incorporation into the PBA framework<sup>21–24</sup> are effective methods for alleviating strain generated during sodium insertion and removal.

Currently, the main anodes being developed for Na-ion batteries are based on metallic Na, carbonaceous materials, conversion phases, and alloys. Although Na metal boasts the highest theoretical capacity at 1165 mAh/g, its performance is severely limited by instability of the SEI and dendrite growth.<sup>25</sup> When considering carbonaceous anodes, graphite would seem an obvious choice given its success as a state-of-the-art anode for Li-ion. However, the large size of Na ions prevents any appreciable intercalation into pristine graphite.<sup>26</sup> In response to this limitation, an ‘‘expanded graphite’’ was developed and reported to deliver a capacity of 280 mAh/g when cycled at C/20 (75% of its theoretical max). Despite this undesirable rate capability, expanded graphite exhibits impressive cyclability, with 74%

capacity retention after 2000 cycles.<sup>27</sup> Hard carbons and doped graphene foam have also been reported as promising anodes, in which surface Na-ion adsorption reportedly adds to interlayer intercalation and results in practical capacities of 431 mAh/g and 220 mAh/g, respectively. However, both these materials suffer from poor stability, fading after only 300 cycles.<sup>28,29</sup> An impressively high capacity of 853 mAh/g was reported for nitrogen-doped graphene foam, attributed to its defect structure and large interlayer spacing, but only 70% of this capacity is retained after 150 cycles.<sup>30</sup> Controlling stress and strain in hard carbon anodes is critical to extending cycle life. Some recent reports on hard carbon anodes investigated strain using in situ imaging techniques to correlate volume expansion to the depth of discharge, uncovering residual strain in the hard carbon after a full charge/discharge cycle.<sup>31</sup> It was hypothesized that this remnant strain could be minimized by controlling the depth of discharge with capacity cutoffs to reduce the overall volume expansion and, in turn, extend the cycling lifetime.<sup>32</sup>

Some of the most heavily characterized anodes exploit conversion reactions and have focused on transition metal sulfides (i.e., MoS<sub>2</sub>, CuS). MoS<sub>2</sub>-carbon composites achieve an impressive practical capacity of 510 mAh/g, however, the capacity retention suffers after only 100 cycles.<sup>33</sup> CuS microflowers exhibit a lower capacity (326 mAh/g), they boast a remarkable cycling lifetime of 5000 cycles, ascribed to their novel nanostructuring and the weakness of *M-S* bonds compared to *M-O* bonds.<sup>34</sup> However, despite this impressive performance, scaling up such a complex nanostructure for implementation in an affordable Na-ion battery is not straightforward.

To balance performance and practicality, alloys are among the most promising anode materials being developed. In general, elements in group 14 and 15 elements (i.e., Si, Ge, Sn, Pb, P, Sb, and Bi) can alloy with Na. Although these materials promise high theoretical capacities, the dramatic crystal structure changes and large volume expansion that occur during alloying often result in poor cycling stability.<sup>35</sup> One notable exception is Sb, which delivers 630 mAh/g at C/5 and retains a capacity of 224 mAh/g after 900 cycles at 3C.<sup>36</sup> Another notable example is nanoporous red phosphorus on reduced graphene oxide (rGO, NPRP@rGO), which achieves an impressive practical capacity of 2110 mAh/g at C/10 (approaching the theoretical capacity).<sup>37</sup> NPRP@rGO maintains a capacity of 775 mAh/g after 1,500 cycles at 2C, thereby exhibiting some of the most promising cycling stability and rate performance. More recently, red phosphorus has been encapsulated in conducting carbons matrices to spatially confine the particle's volume expansion.<sup>37-39</sup> Given the success of these different approaches to accommodate strain in alloy anodes materials, there is great future prospects for red phosphorus and the other classes of candidate anode materials discussed in this overview.<sup>35</sup>

## Impact of structural rigidity

From this brief overview, several trends have emerged, but the major challenge slowing the adoption of practical sodium batteries remains their poor cycle stability. While materials containing large, continuous channels are frequently well-suited for

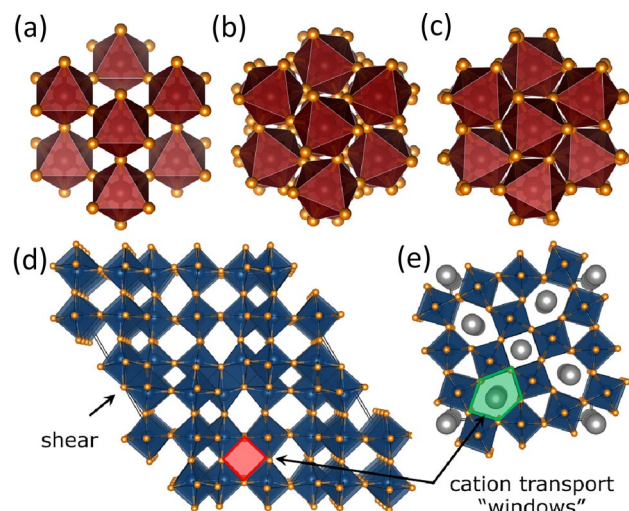


**Figure 2.** Illustration of (a–c) rotational deformation of ReO<sub>3</sub>. Adapted with permission from 40. Copyright 2018 American Chemical Society. (d) Wadsley-Roth TiNb<sub>2</sub>O<sub>7</sub> and (e) tetragonal tungsten bronze Ba<sub>3</sub>Nb<sub>5</sub>O<sub>15</sub>. The triangular motifs observed in the bronzes introduce structural rigidity in the same way as the shear planes in the Wadsley-Roth phases.

ion transport, this alone is not a sufficient condition for Na-ion transport. A prime example of this can be seen in ReO<sub>3</sub>, which boasts a network of three-dimensionally interconnected vacant *A*-sites within the perovskite structure, providing what at first might appear to be ideal channels for Li-ion transport. However, rotation and tilting of the *MO*<sub>6</sub> octahedra results in extremely poor reversibility, with the interpolyhedral angles bending from 180° in the parent structure to 138° in the endmember Li<sub>2</sub>ReO<sub>3</sub> (Fig. 2a–c).<sup>40</sup> This highly localized strain percolates throughout the material and results in particle cracking and delamination of electrodes from the current collector.<sup>41-43</sup>

Hence, one way forward in the development of materials for highly reversible and long-life Na-ion batteries is to develop methods to suppress this type of phase transition during cycling. This is typified by the competitive performance found to date in PBAs. In contrast to the corner-sharing network found in perovskites such as ReO<sub>3</sub>, the cyanide groups that replace oxide ions not only increase the volume of the cavity but can also disrupt the long-range correlations between local tilting distortions that are induced during Na-ion (de)insertion, which allows for modest, reversible capacities to be obtained. Yet, despite the promising performance seen in PBAs, the sensitivity of these materials to incorporation of substitutional water as defects during synthesis creates serious challenges that must be overcome to realize the full potential of this family of materials.<sup>44</sup>

With the goal of creating rigid structures that contain interstitials large enough to host Na with higher capacities, canonical Li-ion hosts can be used as inspiration. Recent reports on fast-cycling Li-ion anode materials demonstrated that crystallographic shear planes in materials, like in the Wadsley-Roth family,<sup>45</sup> reduce the impact of these structural deformations by mechanically locking the structure, thereby enabling both multielectron redox and extremely fast cycling of Li ions.<sup>46-50</sup>

The “locked” structures are formed by a shearing of the corner-connected octahedral network, creating planes of edge-sharing octahedra. While the presence of shear planes reduces the dimensionality of ion transport, it greatly enhances the ion diffusion rate by restricting octahedral tilting and rotation. By optimizing these architectures, high electronic conductivity through the sheared regions and fast Li-ion transport through the connected *A*-sites of the  $\text{ReO}_3$  blocks can be achieved.

Unfortunately, Wadsley-Roth and other shear-phase structures consist primarily of early transition metals with relatively low-lying *d*-orbital levels,<sup>51</sup> resulting in redox potentials better suited for anodes rather than cathodes. More critically, the four-sided channels (highlighted with red in Fig. 2d) found in these shear phases, while sufficient for Li-ion transport, are far too small to accommodate Na-ion diffusion.<sup>52</sup> One class of materials with larger channels that has recently emerged as promising cationic intercalation hosts are the tetragonal tungsten bronzes (TTB),<sup>50,53–56</sup> which contain quite large five-sided tunnels, as illustrated in Fig. 2e. In a way analogous to Wadsley-Roth phases, the triangular motifs in bronzes create these larger five-coordinate channels and, in the process, significantly reduce the ability of the structure to deform during cycling.

### Suppressing glides within layered oxides

Layered Na insertion compounds have among the highest theoretical energy densities of all the candidate cathode materials for Na-ion batteries,<sup>57–62</sup> In analogy with Li-ion cathodes, a promising class of cathode materials for Na-ion batteries is the  $\text{NaMO}_2$  material family, where *M* is a combination of transition metals, with a layered O3 crystal structure (Fig. 3c).<sup>63</sup> In contrast to their Li counterparts, the  $\text{NaMO}_2$  family does not need Co or Ni to stabilize the layered structure and can instead be synthesized with earth-abundant and domestically sourced elements such as Fe and Mn,<sup>64–66</sup> However, simple compounds in this family with only Fe and Mn on the *M* site, such as  $\text{Na}(\text{Fe}_{1-y}\text{Mn}_y)\text{O}_2$ , are suboptimal for commercial applications, as they degrade rapidly when electrochemically cycled and are air and moisture sensitive. Additional transition metals or dopants are required to enhance the cycling performance and mitigate the electrode degradation that occurs due to the significant phase transitions that accompany Na (de)insertion and diffusion.<sup>38,67–69</sup>

The structural transformations that plague layered transition metal oxides and result in severe electrode degradation during Na (de)insertion are best described as changes in the stacking sequence of the two-dimensional  $\text{MO}_2$  building blocks, which induces large and anisotropic shape changes of the electrode particles.<sup>70</sup> This process is schematically illustrated in Fig. 3. The  $\text{NaMO}_2$  intercalation compounds with the highest theoretical energy densities start in the O3 crystal structure but quickly transform to the P3 crystal structure upon Na extraction (Fig. 3c).<sup>30,31,36,38,71–73</sup> The O3 structure exhibits an ABCABC stacking sequence of close-packed anion (oxygen or sulfur) layers, as in an FCC phase, with the alkali and transition metals occupying alternating layers of octahedral sites. Upon removal of 20–30%

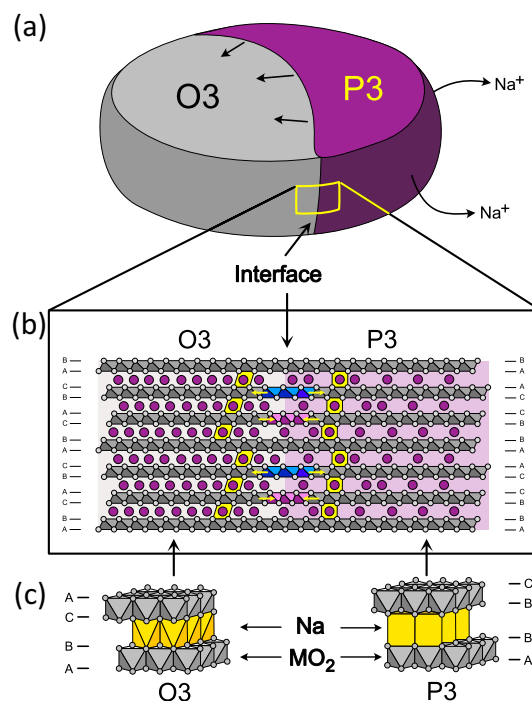


**Figure 3.** Structural phase transformations of layered  $\text{NaMO}_2$  intercalation compounds during Na extraction results in changes in the stacking sequence of the layered  $\text{MO}_2$  building blocks. (a) First-order phase transitions involving a structural transition usually proceed by the passage of a sharp interface separating the growing phase (P3 upon Na extraction) and the phase being consumed (O3). (b) At the crystallographic level, the transition from P3 to O3 can be achieved through a periodic strain field that locally stretches  $\text{MO}_2$  layers in one third of the layers (blue), locally compresses  $\text{MO}_2$  layers in one third of the layers (purple) and leaves the remaining third of  $\text{MO}_2$  layers unstrained. The structural model is one of the many possible mechanisms by which a glide transformation can be realized. (c) The crystal structures of O3 and P3 differ according to the stacking sequence of their  $\text{MO}_2$  sheets. The stacking sequence of the O3 phase produces octahedral sites for Na, whereas that of P3 produces prismatic Na sites.

of the Na, the O3 structure transforms to the P3 structure, which has an ABBCA stacking of the close-packed anion layers, resulting in prismatic coordination of the Na ions (Fig. 3c).

A proposed mechanism for the O3 to P3 structural transition is a glide plane transformation (GPT). However, very little is understood about the mechanisms through which GPTs occur. They require a physical gliding of the atomic planes, leading to substantial chemo-mechanical stresses; moreover, rigid gliding of  $\text{MO}_2$  sheets is an energetically unfavorable process.<sup>74</sup> While there have been no direct observations of glide transitions, a likely mechanism involves the passage of partial dislocations to mediate a change in stacking sequence between adjacent  $\text{MO}_2$  layers.<sup>49,75</sup> However, unlike plastic deformation, where dislocation motion is driven by external mechanical loads, in layered  $\text{NaMO}_2$  compounds they are driven by the chemical force of Na concentration gradients. Figure 3b shows one possible mechanism by which a change in the stacking sequence can be achieved during

the O3 to P3 transition. The rate of this transformation is very sensitive to the diffusion mechanisms of the two phases because the migration of the highly strained interfaces separating O3 from P3 within a single particle is driven by Na-ion diffusion. Na diffusion within the O3 structure, which is mediated by divacancies,<sup>76</sup> is mechanistically very different from that in P3, which has been hypothesized to occur through the migration of anti-phase boundaries that separate well-ordered domains of Na ions.<sup>77-79</sup>

Establishing a fundamental understanding of GPTs is essential to enable the rational design of new layered Na intercalation materials that can attain their full theoretical capacity for many cycles. Careful in situ characterization is critical to understanding the crystallographic and multi-scale mechanisms of GPTs and to informing the development of physics-based, meso-scale models that account for the unique anisotropy of layered materials. Two design strategies will become available upon the development of a mechanistic understanding of GPTs: (i) electrode particles can be designed with sizes and geometries to facilitate elastic and pseudoelastic deformation properties so that GPTs are reversible over thousands of cycles, and (ii) new compositions can be identified that suppress GPTs altogether. Overall, the lack of a mechanistic understanding of glide transitions and the inability to control them is preventing the development of otherwise promising layered Na-ion cathode materials, which are significantly more susceptible to glide transitions than their Li counterparts. Greater fundamental knowledge of these phase transformations is essential to designing electrodes that can achieve their full theoretical capacity, thereby enabling the development of Na-ion batteries with higher energy densities than those currently available and identifying new chemistries for future battery systems.

### Amorphous structures that suppress plastic deformation

Thus far, the cause-and-effect of strain have been discussed solely through the lens of crystalline materials. However, the impact of strain on amorphous materials is also worth exploring due to their lack of long-range order and consequent absence of microstructures. These features contribute to characteristic deformation modes of amorphous materials, which differ from those observed in crystalline materials.<sup>80</sup> For example, while some amorphous materials can be brittle, phases containing metallic bonds are able to accommodate large strains through plastic deformation.<sup>81</sup> These material systems are also known to deflect cracks by facilitating crack branching, which delays material failure.<sup>82</sup> These deformation mechanisms create new pathways for dissipating energy in amorphous materials thereby enabling these materials to accommodate large volume changes without fracture. However, ionic diffusion in amorphous phases is usually slow, thereby requiring compensation via other mechanisms, such as creating nanostructured amorphous electrode materials.

The bonding requirements of amorphous materials precludes their application in some types of electrode materials; for example, highly ionic materials owe their stability to long-range periodicity.

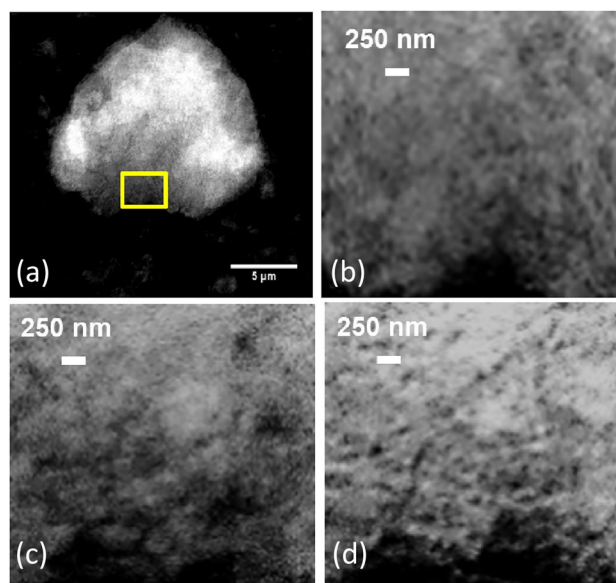


**Figure 4.** TXM images of nanoporous SbSn cycled with lithium: (a, b) full field of view and zoomed-in image, respectively, of a single particle before cycling; (c, d) image of the yellow box in (a) in the fully lithiated and delithiated states, respectively. In all cases, dark dots correspond to nanoscale pores. Excellent retention of the nanoscale structure is observed during alloying a dealloying with Li, a fact that is ascribed both to the two-component nature of the porous material, and to the amorphous nature of the lithiated Sn. Adapted with permission from 90. Copyright 2020 American Chemical Society.

While Na-containing cathodes cannot be easily made amorphous, several anode materials lacking long-range periodicity are known. Among these, two families of materials stand out: alloy anodes and metal oxide hosts. Alloy anodes, in particular, are exciting because of their large capacities,<sup>83,84</sup> but are plagued by large volume change and particle fracturing during cycling which inhibit their long-term cyclability.<sup>85,86</sup> Some improvements in cycling stability can be made through nanostructuring the materials, as structured networks can increase the mechanical flexibility thereby allowing for expansion within the pores that mitigates damage.<sup>87,88</sup> Recent studies on Li-ion anode materials also suggest that amorphous phases can help stabilize structures against cracking. For example, nanoporous antimony tin (NP-SbSn) anodes have been examined using *operando* transmission X-ray microscopy (TXM, see next section for more detail) during (de)lithiation, and show highly reversible deformations of the nanoscale pore system (Fig. 4).<sup>89</sup> This can be ascribed to a combination of the flexible nanoporous structure, the fact that the anode contains two components (Sb and Sn) that alloy with Li at different potentials and thus spread out the volume change, and the fact that the lithiated Sn is observed to be amorphous, providing a more ductile component to the overall composite. In agreement with this idea, in situ hard X-ray nanotomography experiments of lithiated and sodiated bulk Sn powders display differences in volume changes during cycling. The data show the visible formation of large cracks in the primary particles,

and those cracks are influenced by the stresses in the more ductile lithiated tin compared to crystalline sodiated tin.<sup>90</sup>

In considering potential alloy anode materials, elemental Sn, Sb, Ge, Bi, Si, and P have been shown to electrochemically alloy with Li and Na. *Operando* TEM of nanoparticulate Sn revealed that nearly all sodiated intermediates were crystalline.<sup>91–96</sup> Similarly, in situ TEM accompanied by *operando* XRD shows that Bi undergoes a two-step alloying mechanism involving crystalline NaBi and Na<sub>3</sub>Bi.<sup>95</sup> In contrast, Sb, Ge, Si, and certain allotropes of P display amorphous intermediates when cycled versus Na and may show promising behavior.<sup>97–101</sup>

Amorphous phases can also be helpful for oxide-based insertion hosts, and recent results from a group in STORE suggest that TiO<sub>2</sub> is a promising candidate for an amorphous metal oxide host.<sup>102</sup> The abundance of TiO<sub>2</sub>, paired with its environmental and safety advantages make it stand out from other candidate electrode materials with potential to reduce costs in Na-ion batteries. Although there are many scientific reports exploring the use of various polymorphs of this oxide in the field of electrochemistry, the results of Na cycling are inconsistent.

Despite a theoretical capacity of 335 mAh/g (based on the insertion of 1.0 Na-ion per TiO<sub>2</sub> formula unit), TiO<sub>2</sub> polymorphs such as anatase and TiO<sub>2</sub>(B) have shown much lower reversible capacities, rarely exceeded 200 mAh/g when cycled versus Na.<sup>103,104</sup> This is primarily due to the fact that Na-ion intercalation into crystalline TiO<sub>2</sub> phases is thermodynamically unfavorable. However, recent results suggest that amorphous TiO<sub>2</sub> may be a promising anode for Na-ion batteries.<sup>102</sup> When anatase is subjected to Na insertion, it undergoes amorphization in the first 5–10 nm below the surface. A pseudocapacitive charge storage mechanism occurs as Ti<sup>4+</sup>/Ti<sup>3+</sup> redox reactions triggered by Na insertion take place at the surface and near surface regions. 0.8 mol of Na are reversibly (de)intercalated leading to capacities in excess of 250 mAh/g with no evidence of interfacial or conversion reactions. The dramatic improvements in energy and power density when nano-sized anatase is fully converted into the amorphous phase upon sodiation are shown in Fig. 5a for a current density of 1.5 mA/cm<sup>2</sup>. These amorphous nanomaterials also displayed an impressive capacity retention of 90% after 5000 cycles at 3 mA/cm<sup>2</sup> (Fig. 5b). These results show that even in a material as well-known as TiO<sub>2</sub>, there is still much that we do not understand about the nature of Na-ion storage and about the role of amorphization in accommodating insertion-driven strain.

### Materials characterization

As has been discussed extensively, the development and implementation of Na-ion batteries is largely hindered by the structural transformations that accompany Na-ion (de)insertion and diffusion, as these often lead to electrode degradation and poor cycling lifetimes. If Na-ion batteries are to reach large-scale deployment, it will be essential to utilize an extensive array of characterization tools that span multiple time and length scales to better understand the fundamental operating and failure modes of electrodes.

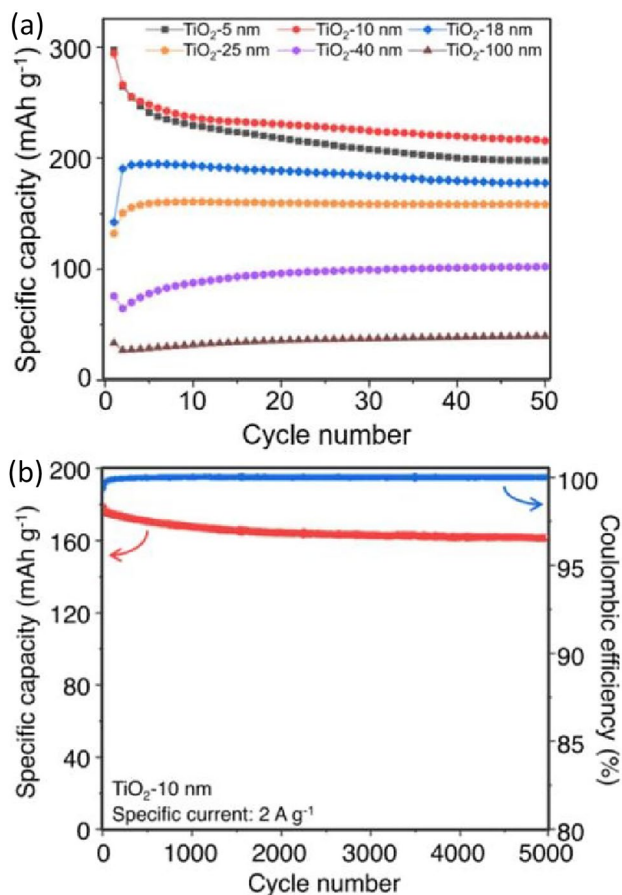
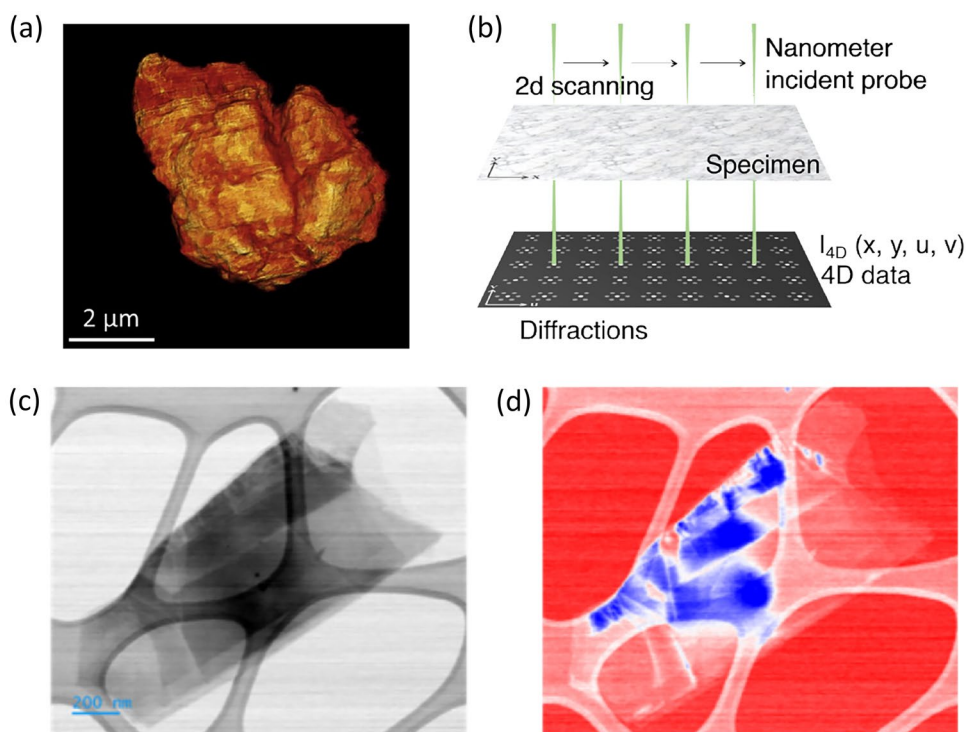


**Figure 5.** (a) Size dependence of the specific capacity showing larger storage with decreasing size of TiO<sub>2</sub> nanoparticles cycled vs sodium at 0.1 A/g. (b) Long-term cycling of 10 nm TiO<sub>2</sub> nanoparticles at 2A/g demonstrating excellent capacity retention after 5000 cycles. Readapted with permission from 104.<sup>102</sup>

At the atomistic level, X-ray absorption near edge structure (XANES) can be used to fingerprint oxidation state changes and provide insights into local coordination environments.<sup>105</sup> Further from the absorption edge, the extended X-ray absorption fine structure (EXAFS) gives insight into the local structure around the absorbing element, even on amorphous materials,<sup>106,107</sup> and by continuously scanning the monochromator, full spectra can be collected in tens of seconds.<sup>108</sup> In conjunction, Raman spectroscopy can be used to monitor changes in metal–ligand bond stiffness or weakening,<sup>109,110</sup> as well as strain, as vibrational modes consistently shift blue under compression and red under tension based on the state of charge.<sup>111</sup>

At the particle level, TXM enables high-resolution (tens of nm) imaging of electrode materials in pouch cells during operation (Fig. 4) and of ex situ electrodes (Fig. 6a). By tuning the incident X-ray energy across an elemental absorption edge, spectroscopic images can be collected to create maps of the chemistry or state of charge. TXM can also be used to track redox changes in metal oxides and sulfides within and between particles during cycling, as well as to directly observe

**Figure 6.** (a) Ex situ X-ray tomography of cracks formed in a SnSb anode particle after 20 cycles. Reprinted from 117, with permission from Elsevier. (b) Schematic illustrating 4D STEM technique. (c) STEM image of pristine graphite particle. (d) Virtual image of the same graphite particle reconstructed by 4D STEM dataset.



morphological changes such as volume expansion, cracking, and pulverization.<sup>65,89,112-115</sup> For example, Fig. 6a shows an example of a reconstructed volume of a single SnSb alloying anode particle that was cycled 20 times versus Li before ex situ data collection, showing the particle cracking that occurs as a result of volume expansion and contraction during cycling.<sup>91</sup> Furthermore, by rotating the sample using a capillary-based cell designed by a team composed of several STORE PIs, nanoscale computed tomography allows for the calculation of quantitative volume and density changes in three dimensions.

Four-dimensional (4D) scanning transmission electron microscopy (STEM) complements TXM studies by providing sub-nanometer spatial resolution by scanning a probe in two-dimensions (2D) and then collecting a 2D diffraction pattern to generate a 4D data cube (Fig. 6b).<sup>116</sup> To stabilize sensitive battery materials under the intense electron beam irradiation required for 4D-STEM, cryogenic conditions are highly beneficial.<sup>117-119</sup> Cryo 4D-STEM is capable of elucidating how strain across a single electrode particle evolves during cycling, providing valuable insights into how crystalline and even amorphous materials degrade at the nanoscale over time.<sup>120-122</sup> For example, in contrast to a real space STEM image (Fig. 6c) of graphite, a virtual image (Fig. 6d) can be reconstructed by probing the electron diffraction image at different locations within the 4D STEM dataset which provides crystallographic information of graphite. The morphology of graphite in virtual image (Fig. 6d) not only matches well with the real image (Fig. 6c), but also has a different contrast from red to blue, highlighting different crystallographic orientations. Furthermore, 4D STEM datasets allow us to calculate small distance changes in the electron diffraction spots and thus generate strain maps induced in the particle after ion intercalation. This new understanding will

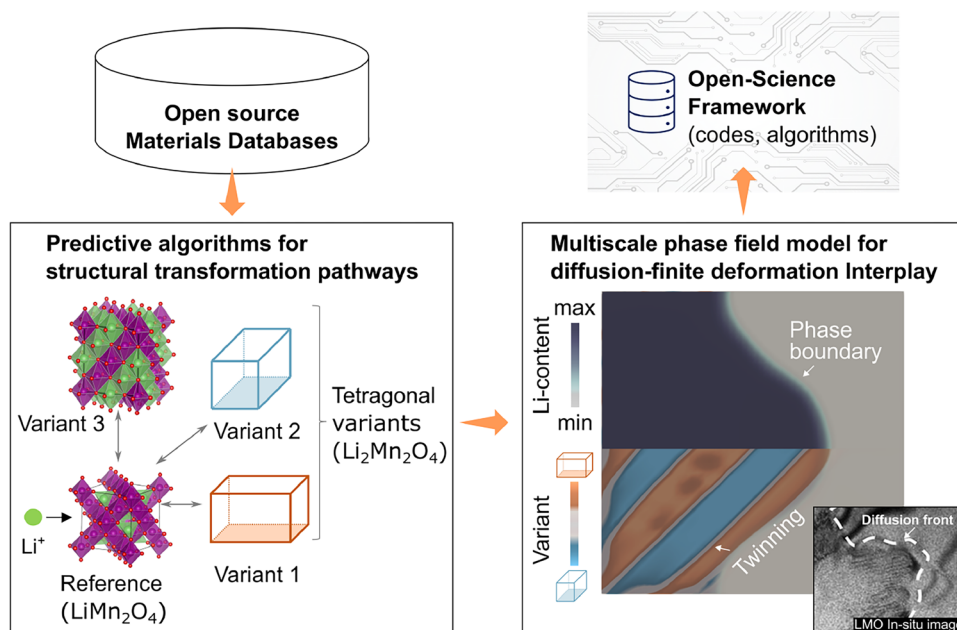
enable the design of materials that can resist strain or distribute it uniformly across particles to mitigate particle degradation during battery operation.

To probe the strain induced during Na insertion at the single particle level, electron transport spectroscopy (ETS)<sup>123-128</sup> can be performed by concurrently measuring the electrical conductance and the electrochemical behavior of a single (or few) particle device. This ultrasensitive on-chip signaling technique could directly determine the sample conductance under varying electrochemical potentials, providing critical information on how lattice strain or phase transition evolves with varying degrees of (de) sodiation states. Clearly, these ex situ and *operando* techniques can be leveraged to establish a greater understanding of the structural and volumetric changes during Na-ion (de)insertion, as well as how materials respond to the strain generated during these processes.

### Theoretical and computational modeling and the role of data science

The reaction of Na with different electrode materials through intercalation or alloying is a multiscale phenomenon, whereby properties at the electronic structure scale greatly impact the material response at the macroscopic scale. The development of integrated multiscale methods and advanced computational models is critical for decoupling many competing effects. Broadly, the computational models in the STORE team can be categorized across atomic and continuum length scales to describe the unique anisotropic chemo-mechanical phenomena observed in intercalation and alloying electrodes.

**Figure 7.** The STORE team is developing a multiscale modeling framework to investigate the interplay between diffusion and lattice deformation in intercalation materials. These models serve as a design tool to engineer the crystallographic texture of intercalation compounds to minimize internal stresses and reduce volume changes during electrochemical cycling.<sup>101–103</sup>



Quantum mechanical simulation techniques based on density functional theory (DFT) and its extensions are remarkably accurate for many material classes. However, predicting the thermodynamic, kinetic, and mechanical properties of battery materials requires simulations that occur on length scales involving millions of atoms and computationally expensive time scales. To address these challenges, the STORE team is developing a first-principles statistical mechanics approach,<sup>74,129</sup> which has been implemented within the CASM software package.<sup>130–132</sup> This approach relies on constructing surrogate models that interpolate first-principles electronic structure calculations within the framework of Monte Carlo and Molecular Dynamics simulations. At the core of these methods is a cluster expansion formalism (a rigorous mathematical approach to construct tunable expansions to describe the energy of a collection of atoms in terms of descriptors of a local environment) that enables the calculation of free energies,<sup>71,133–137</sup> mechanical properties<sup>138–140</sup> and non-dilute diffusion coefficients<sup>76,78,141–147</sup> at finite temperatures starting from first principles. These statistical mechanics techniques are used to calculate the thermodynamic, mechanical, and kinetic properties at finite temperatures, and naturally feed into the phase field and chemo-mechanical continuum models.

Currently, most mesoscale models predict phase transformations in intercalation materials using the guest-species composition (e.g., Li or Na ions) as the order parameter.<sup>148–150</sup> In these methods, lattice deformations are typically homogenized, do not distinguish between lattice variants in symmetry-lowering phase transformations, and are limited in their ability to predict stacking-sequence deformations in layered Na intercalation compounds.<sup>70,151</sup> To address this challenge, STORE PIs have developed new mesoscale models to investigate the interplay between diffusion and finite lattice deformations (see the workflow in Fig. 7); to date the methods have been applied to the  $\text{Li}_x\text{Mn}_2\text{O}_4$  ( $1 < x < 2$ ) system.<sup>152–155</sup> This electro-chemo-mechanical model

reveals fundamental insights into the microstructural evolution pathways under various dynamic galvanostatic conditions and provides quantitative insights into the nucleation and growth of twinned microstructures during intercalation. The results further identify regions of stress concentrations (e.g., at phase boundaries and particle surfaces) that arise from lattice misfit and accumulate in the electrode with repeated cycling and suggest potential mechanisms for the structural decay of  $\text{Li}_2\text{Mn}_2\text{O}_4$ . PIs within the center deposit all codes in repositories like the Open Science Framework (an open-source platform) to facilitate collaboration in materials modeling research.

As the previous sections have discussed, there is a need to develop continuum models to describe diffusion-deformation mechanics, not only in crystalline compounds but also in materials with no long-range order (i.e., amorphous materials). For example, some of the alloy anodes and metal oxide hosts discussed above can involve intermediates that evolve between crystalline and amorphous structures.<sup>58,156</sup> These intermediate compounds are accompanied by enormous volume changes that cause anode materials to crack and/or amorphize and give rise to a plastic-like deformation. In the continuum framework, these changes are analyzed from a microstructural perspective to inform the architecture of electrode materials with porous geometries.

## Conclusion and outlooks

Understanding the fundamental way materials respond to localized strains at the atomic length is a critical first step in the development of highly reversible, long cycle life, Na-ion insertion hosts. As discussed extensively in this perspective, there are a variety of methods that can be employed to mitigate the detrimental effects of large strain. This includes the development

of low strain porous electrode materials, understanding and thereby controlling structural transitions during cycling using experimental and computational analysis techniques, and exploiting the ductility of amorphous phases. Such insights represent the intellectual underpinnings for the creation of more economical and sustainable batteries that could have immediate impact on global energy infrastructure. In pursuing this understanding, open dialogs and close collaborations within interdisciplinary teams will prove critical for developing truly sustainable energy storage solutions.

## Funding

This material is based upon work supported by the U.S. Department of Energy, Office of Science Energy Earthshot Initiative as part of the Center for STRain Optimization for Renewable Energy (STORE) under Award #DE-SC0024730. J.L.A. acknowledges support from the National Science Foundation Graduate Research Fellowship Program under Grant No. DGE-1842487.

## Data Availability

There is no original data in this review, as such this is not applicable for this manuscript

## Declarations

### Competing interests

Not applicable.

## Open Access

This article is licensed under a Creative Commons Attribution 4.0 International License, which permits use, sharing, adaptation, distribution and reproduction in any medium or format, as long as you give appropriate credit to the original author(s) and the source, provide a link to the Creative Commons licence, and indicate if changes were made. The images or other third party material in this article are included in the article's Creative Commons licence, unless indicated otherwise in a credit line to the material. If material is not included in the article's Creative Commons licence and your intended use is not permitted by statutory regulation or exceeds the permitted use, you will need to obtain permission directly from the copyright holder. To view a copy of this licence, visit <http://creativecommons.org/licenses/by/4.0/>.

## REFERENCES

1. X. Xiang, K. Zhang, J. Chen, Recent advances and prospects of cathode materials for sodium-ion batteries. *Adv. Mater.* **27**, 5343–5364 (2015)
2. J.J. Ding, Y.N. Zhou, Q. Sun, X.Q. Yu, X.Q. Yang, Z.W. Fu, Electrochemical properties of P2-phase  $\text{Na}_{0.74}\text{CoO}_2$  compounds as cathode material for rechargeable sodium-ion batteries *Electrochim. Acta* **87**, 388 (2013)

3. D. Su, C. Wang, H.J. Ahn, G. Wang, Single crystalline  $\text{Na}_{0.7}\text{MnO}_2$  nanoplates as cathode materials for sodium-ion batteries with enhanced performance. *Chem. Eur. J.* **19**, 10884 (2013)
4. Y. Yang, Y. Feng, Z. Chen, Y. Feng, Q. Huang, C. Ma, Q. Xia, C. Liang, L. Zhou, M.S. Islam, P. Wang, L. Zhou, L. Mai, W. Wei, Strain engineering by atomic lattice locking in P2-type layered oxide cathode for high-voltage sodium-ion batteries. *Nano Energy* **76**, 105061 (2020)
5. Z. Wu, Y. Ni, S. Tan, E. Hu, L. He, J. Liu, M. Hou, P. Jiao, K. Zhang, F. Cheng, J. Chen, Realizing high capacity and zero strain in layered oxide cathodes via lithium dual-site substitution for sodium-ion batteries. *J. Am. Chem. Soc.* **145**(17), 9596–9606 (2023)
6. J. Hao, J. Zheng, F. Ling, Y. Chen, H. Jing, T. Zhou, L. Fang, M. Zhou, Strain-engineered two-dimensional  $\text{MoS}_2$  as anode material for performance enhancement of Li/Na-ion batteries. *Sci. Rep.* **8**, 2079 (2018)
7. P. Gao, L. Wang, Y. Zhang, Y. Huang, K. Liu, Atomic-scale probing of the dynamics of sodium transport and intercalation-induced phase transformations in  $\text{MoS}_2$ . *ACS Nano* **9**, 11296–11301 (2015)
8. Y. Rao, J. Wang, P. Liang, H. Zheng, M. Wu, J. Chen, F. Shi, K. Yan, J. Liu, K. Bian, C. Zhang, K. Zhu, Heterostructured  $\text{WS}_2/\text{MoS}_2$ @carbon hollow microspheres anchored on graphene for high-performance Li/Na storage. *Chem. Eng. J.* **443**, 136080 (2022)
9. Z. Yuan, J. Cao, S. Valerii, H. Xu, L. Wang, W. Han, MXene-bonded hollow  $\text{MoS}_2$ /carbon sphere strategy for high-performance flexible sodium ion storage. *Chem. Eng. J.* **430**, 132755 (2022)
10. P. Li, J.Y. Jeong, B. Jin, K. Zhang, J.H. Park, Vertically oriented  $\text{MoS}_2$  with spatially controlled geometry on nitrogenous graphene sheets for high-performance sodium-ion batteries. *Adv. Energy Mater.* **8**, 1703300 (2018)
11. X. He, R. Wang, H. Yin, Y. Zhang, W. Chen, S. Huang, 1T- $\text{MoS}_2$  monolayer as a promising anode material for (Li/Na/Mg)-Ion batteries. *Appl. Surf. Sci.* **584**, 152537 (2022)
12. I.V. Chepkasov, M. Ghorbani-Asl, Z.I. Popov, J.H. Smet, A.V. Krashennnikov, Alkali metals inside bi-layer graphene and  $\text{MoS}_2$ : insights from first-principles calculations. *Nano Energy* **75**, 104927 (2020)
13. J. Park, J.-S. Kim, J.-W. Park, T.-H. Nam, K.-W. Kim, J.-H. Ahn, G. Wang, H.-J. Ahn, Discharge mechanism of  $\text{MoS}_2$  for sodium ion battery: electrochemical measurements and characterization. *Electrochim. Acta* **92**, 427–432 (2013)
14. S.Y. Lim, H. Kim, R.A. Shakoor, Y. Jung, J.W. Choi, Electrochemical and thermal properties of NASICON structured  $\text{Na}_3\text{V}_2(\text{PO}_4)_3$  as a sodium rechargeable battery cathode: a combined experimental and theoretical study. *J. Electrochem. Soc.* **159**, A1393 (2012)
15. Y.L. Ruan, K. Wang, S.D. Song, X. Han, B.W. Cheng, Graphene modified sodium vanadium fluorophosphate as a high voltage cathode material for sodium ion batteries. *Electrochim. Acta* **160**, 330 (2015)
16. J. Kim, G. Yoon, M.H. Lee, H. Kim, S. Lee, K. Kang, New 4V-class and zero-strain cathode material for Na-ion batteries. *Chem. Mater.* **29**, 7826–7832 (2017)
17. C. Tealdi, J. Heath, M.S. Islam, Feeling the strain: enhancing ionic transport in olivine phosphate cathodes for Li- and Na-Ion batteries through strain effects. *J. Mater. Chem. A* **4**, 6998–7004 (2016)
18. Y.H. Lu, L. Wang, J.G. Cheng, J.B. Goodenough, Prussian blue: a new framework of electrodes for sodium batteries. *Chem. Commun.* **48**, 6544 (2012)
19. X. Liu, Y. Cao, J. Sun, Defect engineering in prussian blue analogs for high-performance sodium-ion batteries. *Adv. Energy Mater.* **12**, 2202532 (2022)
20. X. Ding, Q. Zhou, Z. Wang, L. Liu, Y. Wang, T. Song, F. Wu, H. Gao, Ultra-stable Mn-based Prussian blue compound effectively

- suppresses Jahn-Teller distortion as superior cathode material for sodium-ion batteries. *J. Mater. Chem. A*, **6**, 12768 (2024)
21. Y. You, X.L. Wu, Y.X. Yin, Y.G. Guo, A zero-strain insertion cathode material of nickel ferricyanide for sodium-ion batteries. *J. Mater. Chem. A*, **1**, 14061–14065 (2013)
  22. B. Xie, P. Zuo, L. Wang, J. Wang, H. Huo, M. He, J. Shu, H. Li, S. Lou, G. Yin, Achieving long-life Prussian blue analogue cathode for Na-ion batteries via triple-cation lattice substitution and coordinated water capture. *Nano Energy* **61**, 201–210 (2019)
  23. F. Gebert, D.L. Cortie, J.C. Bouwer, W. Wang, Z. Yan, S.X. Dou, S.L. Chou, Epitaxial nickel ferrocyanide stabilizes Jahn-Teller distortions of manganese ferrocyanide for sodium-ion batteries. *Angew. Chem.* **133**, 18667–18674 (2021)
  24. L. Shen, Y. Jiang, Y. Jiang, J. Ma, K. Yang, H. Ma, Q. Liu, N. Zhu, Monoclinic bimetallic Prussian blue Analog cathode with high capacity and long life for advanced sodium storage. *ACS Appl. Mater. Interfaces* **14**, 24332–24340 (2022)
  25. J. Zheng, S. Chen, W. Zhao, J. Song, M.H. Engelhard, J.G. Zhang, Extremely stable sodium metal batteries enabled by localized high-concentration electrolytes. *ACS Energy Lett.* **3**, 315–321 (2018)
  26. D.A. Stevens, J.R. Dahn, The mechanisms of lithium and sodium insertion in carbon materials. *J. Electrochem. Soc.* **148**, A803 (2001)
  27. Y. Wen, K. He, Y. Zhu, F. Han, Y. Xu, I. Matsuda, Y. Ishii, J. Cumings, C. Wang, Expanded graphite as superior anode for sodium-ion batteries. *Nat. Commun.* **5**, 4033 (2014)
  28. N. Sun, H. Liu, B. Xu, Facile synthesis of high performance hard carbon anode materials for sodium ion batteries. *J. Mater. Chem. A* **3**, 20560–20566 (2015)
  29. X.F. Luo, C.H. Yang, Y.Y. Peng, N.W. Pu, M.D. Ger, C.T. Hsieh, J.K. Chang, Graphene nanosheets, carbon nanotubes, graphite, and activated carbon as anode materials for sodium-ion batteries. *J. Mater. Chem. A* **3**, 10320–10326 (2015)
  30. J. Xu, M. Wang, N.P. Wickramaratne, M. Jaroniec, S. Dou, L. Dai, High-performance sodium ion batteries based on a 3D anode from nitrogen-doped graphene foams. *Adv. Mater.* **27**, 2042–2048 (2015)
  31. M. Yang, Z. Luo, X. Wang, X. Cao, W. Mao, Y. Pan, C. Dai, J. Pan, Revealing sodium storage mechanism of hard carbon anodes through in-situ investigation of mechano-electrochemical coupling behavior. *J. Energy Chem.* **86**, 227–236 (2023)
  32. F. Xie, Z. Xu, Z. Guo, M.-M. Titirici, Hard carbons for sodium-ion batteries and beyond. *Prog. Energy* **2**, 042002 (2020)
  33. Y.X. Wang, K.H. Seng, S.L. Chou, J.Z. Wang, Z. Guo, D. Wexler, H.K. Liu, S.X. Dou, Reversible sodium storage via conversion reaction of a MoS<sub>2</sub>-C composite. *Chem. Commun.* **50**, 10730–11073 (2014)
  34. C. An, Y. Ni, Z. Wang, X. Li, X. Liu, Facile fabrication of CuS Microflower as a highly durable sodium-ion battery anode. *Inorg. Chem. Front.* **5**, 1045–1052 (2018)
  35. T. Perveen, M. Siddiq, N. Shahzad, R. Ihsan, A. Ahmad, M.I. Shahzad, Prospects in anode materials for sodium ion batteries—A review. *Renew. Sustain. Energy Rev.* **119**, 109549 (2020)
  36. M. Wang, Z. Yang, J. Wang, W. Li, L. Gu, Y. Yu, Sb nanoparticles encapsulated in a reticular amorphous carbon network for enhanced sodium storage. *Small* **11**, 5381–5387 (2015)
  37. S. Liu, H. Xu, X. Bian, J. Feng, J. Liu, Y. Yang, C. Yuan, Y. An, R. Fan, L. Ci, Nanoporous red phosphorus on reduced graphene oxide as superior anode for sodium-ion batteries. *ACS Nano* **12**, 7380–7387 (2018)
  38. L.W. Chen, N. Lu, F. Liu, Y. Shao, L. Wang, Red phosphorus encapsulated in 3D N-doped porous carbon nanofibers: an enhanced sodium-ion battery anode material. *Chem. Commun.* **60**, 3186 (2024)
  39. W. Liu, L. Du, S. Ju, X. Cheng, Q. Wu, Z. Hu, X. Yu, Encapsulation of red phosphorus in carbon nanocages with ultrahigh content for high-capacity and long cycle life sodium-ion batteries. *ACS Nano* **15**(3), 5679–5688 (2021)
  40. N.H. Bashian, S. Zhou, M. Zuba, A.M. Ganose, J.W. Stiles, A. Ee, D.S. Ashby, D.O. Scanlon, L.F.J. Piper, B. Dunn, B.C. Melot, Correlated polyhedral rotations in the absence of polarons during electrochemical insertion of lithium in ReO<sub>3</sub>. *ACS Energy Lett.* **3**, 2513–2519 (2018)
  41. K. Dokko, M. Nishizawa, S. Horikoshi, T. Itoh, M. Mohamedi, I. Uchida, In situ observations of LiNiO<sub>2</sub> single-particle fracture during Li-ion extraction and insertion. *Electrochem. Solid-State Lett.* **3**, 125 (2000)
  42. Y.-I. Jang, B. Huang, H. Wang, D.R. Sadoway, G. Ceder, Y.-M. Chiang, H. Liu, H.J. Tamura, Insights into layered oxide cathodes for rechargeable batteries. *Electrochem. Soc.* **146**, 862–868 (1999)
  43. H. Wang, Y.-I. Jang, B. Huang, D.R. Sadoway, Y.-M. Chiang, TEM study of electrochemical cycling-induced damage and disorder in LiCoO<sub>2</sub> cathode for rechargeable lithium batteries. *J. Electrochem. Soc.* **146**, 473–480 (1999)
  44. Sodium ion Batteries 101: Their Future and Promise. *Benchmark Source: Supply Chain Intelligence for the Energy Transition*. Special Issue 2024.
  45. A.A. Voskanyan, A. Navrotsky, Shear pleasure: the structure, formation, and thermodynamics of crystallographic shear phases. *Ann. Rev. Mater. Res.* **51**, 521–540 (2021)
  46. N.H. Bashian, M.B. Preefer, J. Milam-Guerrero, J.J. Zak, C. Sendi, S.A. Ahsan, R.C. Vincent, R. Haiges, K.A. See, R. Seshadri, B.C. Melot, Understanding the role of crystallographic shear on the electrochemical behavior of niobium oxyfluorides. *J. Mater. Chem. A* **8**, 12623–12632 (2020)
  47. M.B. Preefer, M. Saber, Q. Wei, N.H. Bashian, J.D. Bocarsly, W. Zhang, G. Lee, J. Milam-Guerrero, E.S. Howard, R.C. Vincent, B.C. Melot, A. Van der Ven, R. Seshadri, B.S. Dunn, Multielectron redox and insulator-to-metal transition upon lithium insertion in the fast-charging, Wadsley-roth phase PNB<sub>9</sub>O<sub>25</sub>. *Chem. Mater.* **32**, 4553–4563 (2020)
  48. K.E. Wyckoff, D.D. Robertson, M.B. Preefer, S.L.M. Teicher, J. Bienz, L. Kautzsch, T.E. Mates, J.A. Cooley, S.H. Tolbert, R. Seshadri, High-capacity Li<sup>+</sup> storage through multielectron redox in the fast-charging wadsley-roth phase (W<sub>0.2</sub>V<sub>0.8</sub>)<sub>3</sub>O<sub>7</sub>. *Chem. Mater.* **32**, 9415–9424 (2020)
  49. J.T. Han, J.B. Goodenough, 3-V Full Cell Performance of Anode Framework TiNb<sub>2</sub>O<sub>7</sub>/Spinel LiNi<sub>0.5</sub>Mn<sub>1.5</sub>O<sub>4</sub>. *Chem. Mater.* **23**, 3404–3407 (2011)
  50. K.J. Griffith, K.M. Wiaderek, G. Cibir, L.E. Marbella, C.P. Grey, Niobium tungsten oxides for high-rate lithium-ion energy storage. *Nat.* **559**, 556–563 (2018)
  51. C.M. Hayner, X. Zhao, H.H. Kung, MATERIALS FOR RECHARGEABLE LITHIUM-ION BATTERIES. *Ann. Rev. Chem. Biomol. Eng.* **3**, 445–471 (2012)
  52. K.J. Griffith, I.D. Seymour, M.A. Hope, M.M. Butala, L.K. Lamontagne, M.B. Preefer, C.P. Koçer, G. Henkelman, A.J. Morris, M.J. Cliffe, S.E. Dutton, C.P. Grey, Ionic and electronic conduction in TiNb<sub>2</sub>O<sub>7</sub>. *J. Am. Chem. Soc.* **141**, 16706–16725 (2019)
  53. K.J. Griffith, A.C. Forse, J.M. Griffin, C.P. Grey, High-rate intercalation without nanostructuring in metastable Nb<sub>2</sub>O<sub>5</sub> bronze phases. *J. Am. Chem. Soc.* **138**, 8888–8899 (2016)
  54. L. Yan, X. Cheng, H. Yu, H. Zhu, T. Liu, R. Zheng, R. Zhang, M. Shui, J. Shu, Ultrathin W<sub>9</sub>Nb<sub>8</sub>O<sub>47</sub> nanofibers modified with thermal NH<sub>3</sub> for superior electrochemical energy storage. *Energy Storage Mater.* **14**, 159–168 (2018)
  55. W. Yao, H. Zhu, M. Wang, P. Li, P. Liu, P. Zou, A. Nie, G. Wang, F. Kang, C. Yang, Structural insights into the lithium ion storage behaviors of niobium tungsten double oxides. *Chem. Mater.* **34**, 388–398 (2022)

56. Y. Luo, E. Le Calvez, Y. Zhou, E. Gautron, E. Quarez, M. Preefer, O. Crosnier, J.N. Weker, L. Pilon, T. Brousse, B. Dunn, Structure and electrochemical properties of bronze phase materials containing two transition metals. *Chem. Mater.* **35**, 8675–8685 (2023)
57. C. Delmas, Sodium and sodium-ion batteries: 50 years of research. *Adv. Energy Mater.* **8**, 1703137 (2018)
58. N. Yabuuchi, K. Kubota, M. Dahbi, S. Komaba, Research development on sodium-ion batteries. *Chem. Rev.* **114**, 11636–11682 (2014)
59. M.H. Han, E. Gonzalo, G. Singh, T. Rojo, A comprehensive review of sodium layered oxides: powerful cathodes for Na-ion batteries. *Energy Environ. Sci.* **8**, 81–102 (2015)
60. C. Vaalma, D. Buchholz, M. Weil, S. Passerini, A cost and resource analysis of sodium ion batteries. *Nat. Rev. Mat.* **3**, 1–11 (2018)
61. S. Chu, Y. Zhong, K. Liao, Z. Shao, Layered Co/Ni-free oxides for sodium-ion battery cathode materials. *Curr. Opin. Green Sust. Chem.* **17**, 29–34 (2019)
62. P.-F. Wang, Y. You, Y.-X. Yin, Y.-G. Guo, Layered oxide cathodes for sodium-ion batteries: phase transition, air stability and performance. *Adv. Ener. Mat.* **8**, 1701912 (2018)
63. C. Delmas, C. Fouassier, P. Hagenmuller, Structural classification and properties of the layered oxides. *Physica BC* **99**, 81–85 (1980)
64. B. de Mortemard Boisse, J.-H. Cheng, D. Carlier, M. Guignard, C.-J. Pan, S. Bordere, D. Filimonov, C. Drathen, E. Suard, B.-J. Hwang, A. Wattiaux, C. Delmas, Or- $\text{Na}_x\text{Mn}_{1/3}\text{Fe}_{2/3}\text{O}_2$  as a positive electrode material for Na-ion batteries: structural evolutions and redox mechanisms upon  $\text{Na}^+$  (de)intercalation. *J. Mater. Chem. A* **3**, 10976 (2015)
65. C. Delmas, D. Carlier, M. Guignard, The layered oxides in lithium and sodium-ion batteries: a solid-state chemistry approach. *Adv. Energy Mater.* **11**, 2001201 (2021)
66. Y. Liu, D. Wang, H. Li, P. Li, Y. Sun, Y. Liu, Y. Liu, B. Zhong, Z. Wu, X. Guo, Research progress in O3-type Fe/Mn/Cu-based layered cathode materials for sodium ion batteries. *J. Mater. Chem. A* **10**, 3869 (2022)
67. Y.-K. Sun, Direction for commercialization of O3-Type layered cathodes for sodium-ion batteries. *ACS Energy Lett.* **5**, 1278–1280 (2020)
68. Y. Sun, S. Guo, H. Zhou, Adverse effects of interlayer-gliding in layered transition metal oxides on electrochemical sodium-ion storage. *Energy Environ. Sci.* **12**, 825–840 (2019)
69. K. Wang, P. Yan, M. Sui, Phase transition induced cracking plaguing layered cathode for sodium-ion battery. *Nano Energy* **54**, 148–155 (2018)
70. M.D. Radin, J. Alvarado, Y.S. Meng, A. Van der Ven, Role of crystal symmetry in the reversibility of stacking-sequence changes in layered intercalation electrodes. *Nano Lett.* **17**, 7789–7795 (2017)
71. J. Vinkeviciute, M.D. Radin, A. Van der Ven, Stacking-sequence changes and Na ordering in layered intercalation materials. *Chem. Mater.* **28**, 8640–8650 (2016)
72. M.D. Radin, A. Van der Ven, Stability of prismatic and octahedral coordination in layered oxides and sulfides intercalated with alkali and alkaline-earth metals. *Chem. Mater.* **28**, 7898–7904 (2016)
73. J.L. Kaufman, J. Vinkeviciute, S.K. Kolli, J.G. Goiri, A. Van der Ven, Understanding intercalation compounds for sodium-ion batteries and beyond. *Philos. Trans. Royal Soc. A* **377**, 20190020 (2019)
74. A. Van der Ven, Z. Deng, S. Banerjee, S.P. Ong, Rechargeable alkali-ion battery materials: theory and computation. *Chem. Rev.* **120**, 6977–7019 (2020)
75. H. Gabrisch, R. Yazami, B. Fultz, The character of dislocations in  $\text{LiCoO}_2$ . *Electrochem. Solid State Lett.* **5**, A111 (2002)
76. A. Van der Ven, J. Bhattacharya, A.A. Belak, Understanding Li diffusion in Li-intercalation compounds. *Acc. Chem. Res.* **46**, 1216–1225 (2013)
77. J.L. Kaufman, A. Van der Ven, Antiphase boundary migration as a diffusion mechanism in a P3 sodium layered oxide. *Phys. Rev. Mater.* **5**, 055401 (2021)
78. J.L. Kaufman, A. Van der Ven, Cation diffusion facilitated by antiphase boundaries in layered intercalation compounds<sup>†</sup>. *Chem. Mater.* **34**, 1889–1896 (2022)
79. J.L. Kaufman, A. Van der Ven,  $\text{Na}_x\text{CoO}_2$  phase stability and hierarchical orderings in the O3/P3 structure family. *Phys. Rev. Mater.* **3**, 015402 (2019)
80. M.L. Falk, J.S. Langer, Deformation and failure of amorphous, solidlike materials. *Annu. Rev. Condens. Matter Phys.* **2**, 353–373 (2011)
81. C.A. Schuh, T.C. Hufnagel, U. Ramamurty, Mechanical behavior of amorphous alloys. *Acta Mater.* **55**, 4067–4109 (2007)
82. I.S. Aranson, V.A. Kalatsky, V.M. Vinokur, Continuum field description of crack propagation. *Phys. Rev. Lett.* **85**, 118 (2000)
83. W.-J. Zhang, A review of the electrochemical performance of alloy anodes for lithium-ion batteries. *J. Power. Sources* **196**, 13–24 (2011)
84. Y. Zhao, A. Manthiram, High-capacity, high-rate, Bi-Sb alloy anodes for lithium-ion and sodium-ion batteries. *Chem. Mater.* **27**, 3096–3101 (2015)
85. M.N. Obrovac, L. Christensen, B.L. Le, J.R. Dahn, Alloy design for lithium-ion battery anodes. *J. Electrochem. Soc.* **154**, A849 (2007)
86. W.-J. Zhang, Lithium insertion/extraction mechanism in alloy anodes for lithium-ion batteries. *J. Power. Sources* **196**, 877–885 (2011)
87. T. Wada, T. Ichitsubo, K. Yubuta, H. Segawa, H. Yoshida, H. Kato, Bulk-nanoporous-silicon negative electrode with extremely high cyclability for lithium-ion batteries prepared using a top-down process. *Nano Lett.* **14**, 4505–4510 (2014)
88. J.B. Cook, T.C. Lin, E. Detsi, J. Nelson Weker, S.H. Tolbert, Using X-ray microscopy to understand how nanoporous materials can be used to reduce the large volume change in alloy anodes. *Nano Lett.* **17**, 870–877 (2017)
89. T.C. Lin, A. Dawson, S.C. King, Y. Yan, D.S. Ashby, J.A. Mazzetti, B.S. Dunn, J. Nelson Weker, S.H. Tolbert, Understanding stabilization in nanoporous intermetallic alloy anodes for Li-Ion batteries using operando transmission X-ray microscopy. *ACS Nano* **14**, 14820–14830 (2020)
90. J. Wang, C. Eng, Y.C. Chen-Wiegart et al., Probing three-dimensional sodiation–desodiation equilibrium in sodium-ion batteries by in situ hard X-ray nanotomography. *Nat. Commun.* **6**, 7496 (2015)
91. L.D. Ellis, T.D. Hatchard, M.N. Obrovac, Reversible Insertion of Sodium in Tin. *J. Electrochem. Soc.* **159**, A1801 (2012)
92. A. Darwiche, C. Marino, M.T. Sougrati, B. Fraise, L. Stievano, L. Monconduit, Better cycling performances of bulk Sb in Na-Ion batteries compared to li-ion systems: an unexpected electrochemical mechanism. *J. Am. Chem. Soc.* **134**, 20805–20811 (2012)
93. X. Lu, E.R. Adkins, Y. He, L. Zhong, L. Luo, S.X. Mao, C.M. Wang, B.A. Korgel, Germanium as a sodium ion battery material. In situ TEM reveals fast sodiation kinetics with high capacity. *Chem. Mater.* **28**, 1236–1242 (2016)
94. Y. Han, N. Lin, T. Xu, T. Li, J. Tian, Y. Zhu, Y. Qian, An amorphous Si material with a sponge-like structure as an anode for Li-ion and Na-ion batteries. *Nanoscale* **10**, 3153–3158 (2018)
95. C. Wang, L. Wang, F. Li, F. Cheng, J. Chen, Bulk bismuth as a high-capacity and ultralong cycle-life anode for sodium-ion batteries by coupling with Glyme-based electrolytes. *Adv. Mater.* **29**, 1702212 (2017)
96. L. Baggetto, P. Ganesh, R.P. Meisner, R.R. Unocic, J.-C. Jumas, C.A. Bridges, G.M. Veith, Characterization of sodium ion

- electrochemical reaction with tin anodes: experiment and theory. *J. Power. Sources* **234**, 48 (2013)
97. P.K. Allan, J.M. Griffin, A. Darwiche, O.J. Borkiewicz, K.M. Wiaderek, K.W. Chapman, A.J. Morris, P.J. Chupas, L. Monconduit, C.P. Grey, Tracking sodium-antimonide phase transformations in sodium-ion anodes: insights from operando pair distribution function analysis and solid-state NMR spectroscopy. *J. Am. Chem. Soc.* **138**, 2352–2365 (2016)
  98. P.R. Abel, Y.-M. Lin, T. de Souza, C.-Y. Chou, A. Gupta, J.B. Goodenough, G.S. Hwang, A. Heller, C.B. Mullins, Nanocolumnar germanium thin films as a high-rate sodium-ion battery anode material. *J. Phys. Chem. C* **117**, 18885–18890 (2013)
  99. F.-H. Du, L. Zhang, Y.-C. Tang, S.-Q. Li, Y. Huang, L. Dong, Q. Li, H. Liu, D. Wang, Y. Wang, Low-temperature synthesis of amorphous silicon and its ball-in-ball hollow nanospheres as high-performance anodes for sodium-ion batteries. *Adv. Mater. Interfaces* **9**, 2102158 (2022)
  100. G.L. Xu, Z. Chen, G.M. Zhong, Y. Liu, Y. Yang, T. Ma, Y. Ren, X. Zuo, X.H. Wu, X. Zhang, K. Amine, Nanostructured black phosphorus/Ketjenblack–Multiwalled carbon nanotubes composite as high-performance anode material for sodium-ion batteries. *Nano Lett.* **16**, 3955–3965 (2016)
  101. L.E. Marbella, M.L. Evans, M.F. Groh, J. Nelson, K.J. Griffith, A.J. Morris, C.P. Grey, Sodiation and desodiation via helical phosphorus intermediates in high-capacity anodes for sodium-ion batteries. *J. Am. Chem. Soc.* **140**, 7994–8004 (2018)
  102. Q.L. Wei, X. Chang, D. Butts, R. DeBlock, K. Lan, J. Li, D. Chao, D.-L. Peng, B. Dunn, Surface-redox sodium-ion storage in anatase titanium oxide. *Nat. Commun.* **14**, 7 (2023)
  103. L. Shen, K. Niu, S. Chen, X. Sun, L. Liu, B. Jiang, L. Chu, X. Lv, M. Li, TiO<sub>2</sub> bunched hierarchical structure with effective enhancement in sodium storage behaviors. *Carbon Energy* **4**, 645–653 (2022)
  104. S. Liang, X. Wang, Y. Cheng, Y. Xia, P. Müller-Buschbaum, Anatase titanium dioxide as rechargeable ion battery electrode - A chronological review. *Energy Storage Mater.* **45**, 201–264 (2022)
  105. T. Yamamoto, Assignment of pre-edge peaks in K-edge x-ray absorption spectra of 3d transition metal compounds: Electric dipole or quadrupole? *X-Ray Spectrometry: X-Ray Spectrom.* **37**, 572–584 (2008)
  106. L.Y. Lim, N. Liu, Y. Cui, M.F. Toney, Understanding phase transformation in crystalline Ge anodes for Li-Ion batteries. *Chem. Mater.* **26**, 3739–3746 (2014)
  107. L.C. Loaiza, N. Louvain, B. Fraisse, A. Boulaoued, A. Iadecola, P. Johansson, L. Stievano, V. Seznec, L. Monconduit, Electrochemical lithiation of Ge: new insights by operando spectroscopy and diffraction. *J. Phys. Chem. C* **122**, 3709–3718 (2018)
  108. O. Müller, M. Nachttegaal, J. Just, D. Lützenkirchen-Hecht, R. Frahm, Quick-EXAFS setup at the SuperXAS beamline for in situ X-ray absorption spectroscopy with 10 ms time resolution. *J. Synchrotron Radiat.* **23**, 260–266 (2016)
  109. J.J. Zak, M. Zuba, Z.W. Lebens-Higgins, H. Huang, M.J. Crafton, N.F. Dalleska, B.D. McCloskey, L.F.J. Piper, K.A. See, Irreversible anion oxidation leads to dynamic charge compensation in the Ru-Poor, Li-rich cathode Li<sub>2</sub>Ru<sub>0.3</sub>Mn<sub>0.7</sub>O<sub>3</sub>. *ACS Energy Lett.* **8**, 722–730 (2022)
  110. K.E. Wyckoff, J.L. Kaufman, S.W. Baek, C. Dolle, J.J. Zak, J. Bienz, L. Kautzsch, R.C. Vincent, A. Zohar, K.A. See, Y.M. Eggeler, L. Pilon, A. Van der Ven, R. Seshadri, Metal-metal bonding as an electrode design principle in the low-strain cluster compound LiScMo<sub>3</sub>O<sub>8</sub>. *J. Am. Chem. Soc.* **144**, 5841–5854 (2022)
  111. R.J. Angel, M. Murri, B. Mihailova, M. Alvaro, Stress, strain and Raman shifts. *Z. Für Krist. - Cryst. Mater.* **234**, 129–140 (2019)
  112. J. Nelson Weker, A.M. Wise, K. Lim, B. Shyam, M.F. Toney, Operando spectroscopic microscopy of LiCoO<sub>2</sub> cathodes outside standard operating potentials. *Electrochim. Acta* **247**, 977–982 (2017)
  113. J. Nelson Weker, Y. Li, R. Shanmugam, W. Lai, W.C. Chueh, Tracking non-uniform mesoscale transport in LiFePO<sub>4</sub> agglomerates during electrochemical cycling. *ChemElectroChem* **2**, 1576–1581 (2015)
  114. S.S. Kim, D.N. Agyeman-Budu, J.J. Zak, A. Dawson, Q. Yan, M. Cában-Acevedo, K.M. Wiaderek, A.A. Yakovenko, Y. Yao, A. Irshad, S.R. Narayan, J. Luo, J. Nelson Weker, S.H. Tolbert, K.A. See, Promoting reversibility of multielectron redox in Alkali-rich sulfide cathodes through cryomilling. *Chem. Mater.* **34**, 3236–3245 (2022)
  115. Q. Yan, S.-T. Ko, A. Dawson, D. Agyeman-Budu, G. Whang, Y. Zhao, M. Qin, B.S. Dunn, J. Nelson Weker, S.H. Tolbert, J. Luo, Thermodynamics-driven interfacial engineering of alloy-type anode materials. *Cell Rep. Physical Science* **3**, 100694 (2022)
  116. K.C. Bustillo, S.E. Zeltmann, M. Chen, J. Donohue, J. Ciston, C. Ophus, A.M. Minor, 4D-STEM of beam-sensitive materials. *Acc. Chem. Res.* **54**, 2543–2551 (2021)
  117. Y. Li, Y. Li, A. Pei, K. Yan, Y. Sun, C. Wu, L. Joubert, R. Chin, A. Koh, Y. Yu, J. Perrino, B. Butz, S. Chu, Y. Cui, Atomic structure of sensitive battery materials and interfaces revealed by cryo-electron microscopy. *Science* **358**, 506–510 (2017)
  118. Z. Zhang, Y. Li, R. Xu, W. Zhou, Y. Li, S.T. Oyakhire, Y. Wu, J. Xu, H. Wang, Z. Yu, D.T. Boyle, W. Huang, Y. Ye, H. Chen, J. Wan, Z. Bao, W. Chiu, Y. Cui, Capturing the swelling of solid-electrolyte interphase in lithium metal batteries. *Science* **375**, 66–70 (2022)
  119. Y. Li, W. Huang, Y. Li, W. Chiu, Y. Cui, Opportunities for cryogenic electron microscopy in materials science and nanoscience. *ACS Nano* **14**, 9263–9276 (2020)
  120. W. Chen, X. Zhan, R. Yuan, S. Pidaparthy, A.X.B. Yong, H. An, Z. Tang, K. Yin, A. Patra, H. Jeong, C. Zhang, K. Ta, Z.W. Riederl, R.M. Stephens, D.P. Shoemaker, H. Yang, A.A. Gewirth, P.V. Braun, E. Ertekin, J.M. Zuo, Q. Chen, Formation and impact of nanoscopic oriented phase domains in electrochemical crystalline electrodes. *Nat. Mater.* **22**, 92–99 (2023)
  121. C. Mahr, K. Muller-Caspary, T. Grieb, F.F. Krause, M. Schowalter, A. Rosenauer, Accurate measurement of strain at Interfaces in 4D-STEM: a comparison of various methods. *Ultramicroscopy* **221**, 113196 (2021)
  122. C. Gammer, C. Ophus, T.C. Pekin, J. Eckert, A.M. Minor, Local nanoscale strain mapping of a metallic glass during in situ testing. *Appl. Phys. Lett.* **112**, 171905 (2018)
  123. C. Wang, Q. He, U. Halim, Y. Liu, E. Zhu, Z. Lin, H. Xiao, X.D. Duan, Z. Feng, R. Cheng, N. Weiss, G. Ye, Y.C. Huang, H. Wu, H.-C. Cheng, I. Shakir, L. Liao, X. Chen, W.A. Goddard, Y. Huang, X. Duan, Monolayer atomic crystal molecular superlattices. *Nature* **555**, 231–236 (2018)
  124. T. He, W. Wang, F. Shi, X. Yang, X. Li, J. Wu, Y. Yin, M. Jin, Mastering the surface strain of platinum catalysts for efficient electrocatalysis. *Nature* **598**, 76–81 (2021)
  125. W. Zuo, X. Liu, J. Qiu, D. Zhang, Z. Xiao, J. Xie, F. Ren, J. Wang, Y. Li, G.F. Ortiz, W. Wen, S. Wu, M.-S. Wang, R. Fu, Y. Yang, Engineering Na<sup>+</sup>-layer spacings to stabilize Mn-based layered cathodes for sodium-ion batteries. *Nat. Commun.* **12**, 4903 (2021)
  126. Q. He, Z. Lin, M. Ding, A. Yin, U. Halim, C. Wang, Y. Liu, H.-C. Cheng, Y. Huang, X. Duan, In situ probing molecular intercalation in two-dimensional layered semiconductors. *Nano Lett.* **19**, 6819–6826 (2019)
  127. G. Zhong, T. Cheng, A.H. Shah, C. Wan, Z. Huang, S. Wang, T. Leng, Y. Huang, W.A. Goddard III., X. Duan, Determining the hydronium pK<sub>a</sub> at platinum surfaces and the effect on pH-dependent hydrogen evolution reaction kinetics. *Proc. Natl. Acad. Sci. U.S.A.* **119**, e2208187119 (2022)

128. A.H. Shah, Z. Zhang, Z. Huang, S. Wang, G. Zhong, C. Wan, A.N. Alexandrova, Y. Huang, X. Duan, The role of alkali metal cations and platinum-surface hydroxyl in the alkaline hydrogen evolution reaction. *Nat. Catal.* **5**, 923–933 (2022)
129. A. Van der Ven, J.C. Thomas, B. Puchala, A.R. Natarajan, First-principles statistical mechanics of multicomponent crystals. *Annu. Rev. Mater. Res.* **48**, 27–55 (2018)
130. B. Puchala, J.C. Thomas, A.R. Natarajan, J.G. Goiri, S.S. Behara, J.L. Kaufman, A. Van der Ven, CASM – A software package for first-principles based study of multicomponent crystalline solids. *Comput. Mater. Sci.* **217**, 111897 (2023)
131. “CASM documentation.” [https://prisms-center.github.io/CASMc ode\\_docs/](https://prisms-center.github.io/CASMc ode_docs/), 2023.
132. Van der Ven Research Group, “CASM: A clusters approach to statistical mechanics.” <https://github.com/prisms-center/CASMc ode>, 2023.
133. A.R. Natarajan, J.C. Thomas, B. Puchala, A. Van der Ven, Symmetry-adapted order parameters and free energies for solids undergoing order-disorder phase transitions. *Phys. Rev. B* **96**, 134204 (2017)
134. J.L. Kaufman, J. Vinkeviciute, S. Krishna Kolli, J. Gabriel Goiri, A. Van der Ven, Understanding intercalation compounds for sodium-ion batteries and beyond. *Phil. Trans. R. Soc. A* **377**, 20190020 (2019)
135. G.H. Teichert, A.R. Natarajan, A. Van der Ven, K. Garikipati, Active learning workflows and integrable deep neural networks for representing the free energy functions of alloys. *Comput. Methods Appl. Mech. Eng.* **371**, 113281 (2020)
136. G.H. Teichert, A.R. Natarajan, A. Van der Ven, K. Garikipati, Machine learning materials physics: Integrable deep neural networks enable scale bridging by learning free energy functions. *Comput. Methods Appl. Mech. Eng.* **353**, 201–216 (2019)
137. G.H. Teichert, N.S.H. Gunda, S. Rudraraju, A.R. Natarajan, B. Puchala, K. Garikipati, A. Van der Ven, A comparison of Redlich-Kister polynomial and cubic spline representations of the chemical potential in phase field computations. *Comput. Mater. Sci.* **128**, 127–139 (2017)
138. J.C. Thomas, A. Van der Ven, The exploration of nonlinear elasticity and its efficient parameterization for crystalline materials. *J. Mech. Phys. Solids* **107**, 76–95 (2017)
139. J.C. Thomas, A. Van der Ven, Elastic properties and stress-temperature phase diagrams of high-temperature phases with low-temperature lattice instabilities. *Phys. Rev. B* **90**, 224105 (2014)
140. A.R. Natarajan, A. Van der Ven, Linking electronic structure calculations to generalized stacking fault energies in multicomponent alloys. *Npj Comput. Mater.* **6**, 80 (2020)
141. S.K. Kolli, A. Van der Ven, Elucidating the factors that cause cation diffusion shutdown in spinel-based electrodes. *Chem. Mater.* **33**, 6421–6432 (2021)
142. J.G. Goiri, S.K. Kolli, A. Van der Ven, Role of short-and long-range ordering on diffusion in Ni-Al alloys. *Phys. Rev. Mater.* **3**, 093402 (2019)
143. J. Bhattacharya, A. Van der Ven, First-principles study of competing mechanisms of nondilute Li diffusion in spinel  $\text{Li}_x\text{TiS}_2$ . *Phys. Rev. B* **83**, 144302 (2011)
144. J. Bhattacharya, A. Van der Ven, Phase stability and nondilute Li diffusion in spinel  $\text{Li}_{1+x}\text{Ti}_2\text{O}_4$ . *Phys. Rev. B* **81**, 104304 (2010)
145. A. Van der Ven, H.-C. Yu, G. Ceder, K. Thornton, Vacancy mediated substitutional diffusion in binary crystalline solids. *Prog. Mater. Sci.* **55**, 61–105 (2010)
146. A. Van der Ven, J.C. Thomas, Q. Xu, B. Swoboda, D. Morgan, Nondilute diffusion from first principles: Li diffusion in  $\text{Li}_x\text{TiS}_2$ . *Phys. Rev. B* **78**, 104306 (2008)
147. A. Van der Ven, G. Ceder, M. Asta, P. Tepesch, First-principles theory of ionic diffusion with nondilute carriers. *Phys. Rev. B* **64**, 184307 (2001)
148. P. Ombrini, M.Z. Bazant, M. Wagemaker, Vasileiadis, A; Thermodynamics of multi-sublattice battery active materials: from an extended regular solution theory to a phase-field model of  $\text{LiMn}_y\text{Fe}_{1-y}\text{PO}_4$ . *Npj Comput. Mater.* **9**, 148 (2023)
149. D. Zhang, J. Sheth, B.W. Sheldon, A.R. Balakrishna, Film strains enhance the reversible cycling of intercalation electrodes. *J. Mech. Phys. Solids* **155**, 104551 (2021)
150. A. Renuka Balakrishna, Crystallographic design of intercalation materials. *J. Electrochem. En. Conv. Stor.* **19**, 040802 (2022)
151. T. Erichsen, B. Pfeiffer, V. Roddatis, C.A. Volkert, Tracking the diffusion-controlled lithiation reaction of  $\text{LiMn}_2\text{O}_4$  by in situ tem. *ACS Appl. Energy Mater.* **3**, 5405–5414 (2020)
152. T. Zhang, D. Zhang, A.R. Balakrishna, Coupling diffusion and finite deformation in phase transformation materials. *J. Mech. Phys. Solids* **183**, 105501 (2024)
153. D. Zhang, A.R. Balakrishna, Designing shape-memory-like microstructures in intercalation materials. *Acta Mater.* **252**, 118879 (2023)
154. A.R. Balakrishna, W.C. Carter, Combining phase-field crystal methods with a Cahn-Hilliard model for binary alloys. *Phys. Rev. E* **97**, 043304 (2018)
155. A.R. Balakrishna, Y.M. Chiang, W.C. Carter, Phase-field model for diffusion-induced grain boundary migration: an application to battery electrodes. *Phys. Rev. Mater.* **3**, 065404 (2019)
156. D. Chang, H. Huo, K.E. Johnston, M. Ménétrier, L. Monconduit, A. Van der Ven, Elucidating the origins of phase transformation hysteresis during electrochemical cycling of Li–Sb electrodes. *J. Mater. Chem. A* **3**, 18928–18943 (2019)

**Publisher's Note** Springer Nature remains neutral with regard to jurisdictional claims in published maps and institutional affiliations.